European Journal of Computational Mechanics, 2013
Vol. 22, Nos. 2–4, 228–235, http://dx.doi.org/10.1080/17797179.2013.820895

Thermo-mechanical fatigue design of automotive heat exchangers

Frédéric Roger* and Alexander Chidley

Unité de Mécanique, ENSTA Paristech, Chemin de la Hunière, Palaiseau 91120, France

Automotive heat exchangers are manufactured using brazed thin aluminium tubes and are submitted to pressure pulses, thermal shocks and corrosion. Thermal shocks induce low cycle thermo-mechanical fatigue that leads to failure after several thousand cycles. We propose a thermo-mechanical fatigue design approach for automotive heat exchangers based on the experimental identification of the thermal history during the thermal shock by infrared thermography, the identification of the cyclic elasto-plastic behaviour of the brazed aluminium tubes and the development of a multiaxial lifetime criteria. A finite element simulation of the cyclic thermo-mechanical response in the critical area of the heat exchanger and the use of a multiaxial energy based lifetime criteria lead to the prediction of the heat exchanger's life.

Keywords: thermal fatigue; automotive heat exchanger; infrared thermography; nanoindentation; finite element

1. Introduction

Automotive heat exchangers are manufactured using aluminium tubes brazed to fins to dissipate heat from the cooling fluid. The aluminium tubes are made from aluminium laminate having three layers; the central layer is a 3916 aluminium alloy, whilst the outside layers are made from 4045 aluminium alloy chosen for its brazing capability and corrosion protection.

These thin structures are submitted to thermal shock up to 110 °C which induces plasticity in the critical zones of the heat exchanger. After several thousands of thermal shocks, low cycle thermal fatigue leads to failure. In order to optimise the design of new automotive heat exchangers, it is necessary to predict the cyclic thermo-mechanical response and the heat exchanger's life duration. In the present study, we propose a constitutive approach for the fatigue design of the heat exchanger under thermal shock conditions.

The first part is dedicated to the identification of the thermal history in the thin tubes during a thermal shock test using sequentially 35 and 110 °C cooling fluids. In the second part, we propose a cyclic elasto-plastic model of the aluminium laminate. The third part proposes a numerical simulation of the critical part of the heat exchanger under cyclic thermal shocks to illustrate our thermal fatigue design approach.

*Corresponding author. Email: frederic.roger@ensta-paristech.fr

2. Thermal history of the exchanger during a thermal shock test

Both cool and hot fluids (35 and 110 °C) are cyclically distributed through a brazed cross-flow heat exchanger. An infrared thermography camera is used with several lens sizes to register the thermal cycles in the tubes and to monitor the temperature map. Following calibration of the emissivity, the temperature distribution in the heat exchanger during a shock appears as shown in Figure 1. Figure 2 illustrates graphically the thermal cycles for the three points located close to the inlet side of the exchanger as defined in Figure 1. From the thermal cycles, we propose a dimensionless form for $T/T_{\max}$ as defined in Equation (1).

$$\frac{T}{T_{max}} = \frac{\tan^{-1}(t - t_0)}{\pi} + \frac{1}{2} \tag{1}$$

As an alternative to modelling the fluid flow and heat transfer within the heat exchanger, this in order to predict thermal history, infrared thermography is used, this providing data in a form that can be used directly in thermo-mechanical simulations.

3. Cyclic elasto-plastic behaviour of the aluminium laminate

Each tube is manufactured from an aluminium laminate of 200 µm thickness having three layers (4045-3916-4045) and is subsequently brazed to fins. During brazing, silicon contained within the outside layers diffuses towards the heart layer, and recrystallisation is observed. Microhardness tests show a slight hardness gradient across the thickness of the brazed laminate. Tensile tests for brazed aluminium laminate specimens cut in longitudinal and transverse lamination directions, show that after brazing the behaviour is isotropic.

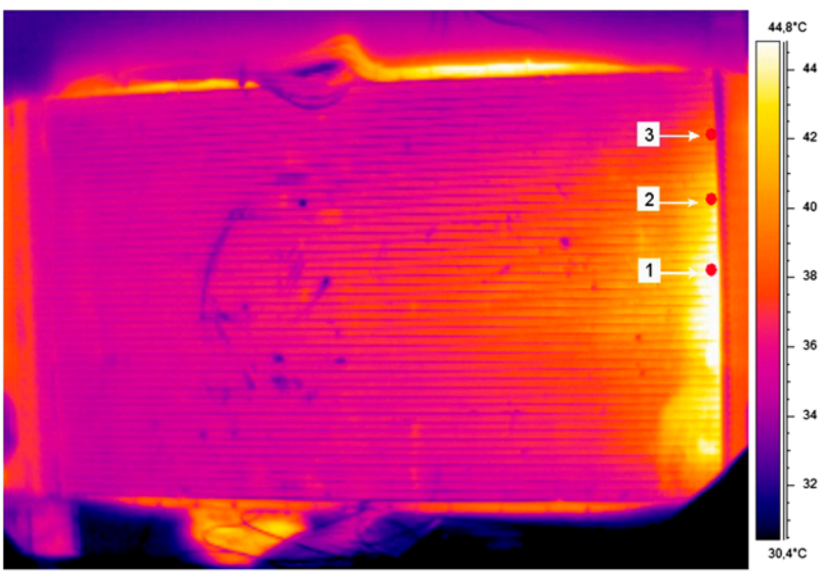

Figure 1. Thermal map of the heat exchanger, when the hot fluid fills the right side ($t = 62$ s).

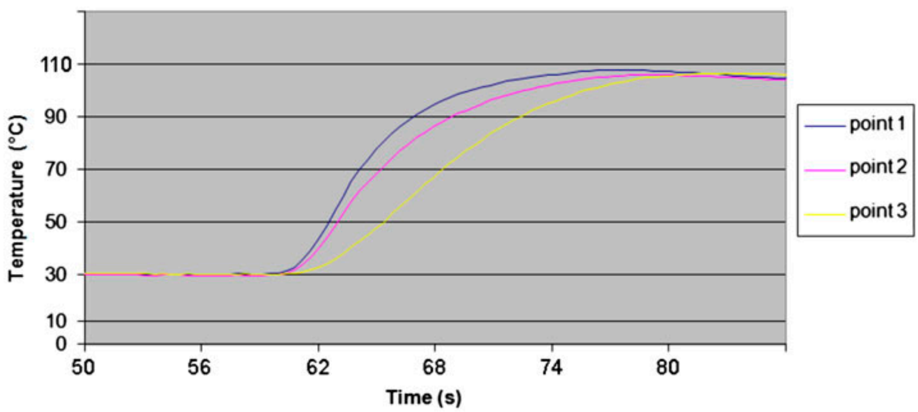

Figure 2. Thermal cycles for three points located in the inlet side as defined in Figure 1.

The slender nature of the tubes and subsequent risk of buckling does not allow any possibility of effecting tensile/compression tests to identify the cyclic hardening type. We decided to identify the hardening type by cyclic tensile/compression testing a thick specimen of 3916 aluminium alloy.

Figure 3 shows the cyclic response of the specimen. The cyclic hardening is identified as a combined isotropic and non-linear kinematic hardening.

We propose to use the combined hardening Chaboche elasto-plastic model with a non linear kinematic hardening (Chaboche, 1989), where the governing equations are as follows:

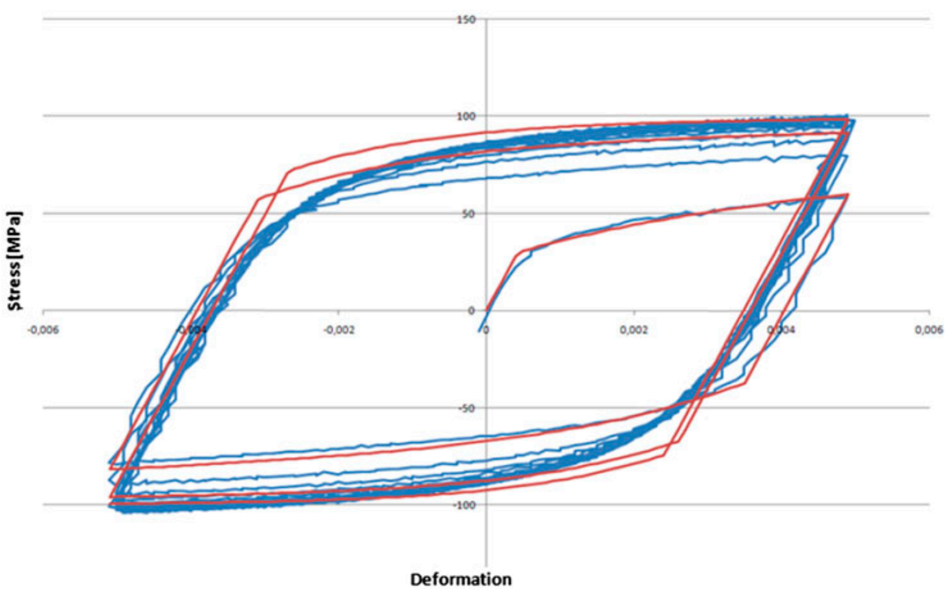

Figure 3. Cyclic mechanical response during the test (blue) and corresponding curve (red) for a combined hardening after identification.

$$\sigma = \left(K - \frac{2}{3}G\right)Tr(\varepsilon - \varepsilon_{\mathrm{p}})1 + 2G(\varepsilon - \varepsilon_{\mathrm{p}}) \tag{2}$$

$$f = J_2(\sigma - X) - R - \sigma_y \tag{3}$$

$$R = Q(1 - e^{-bp}) \tag{4}$$

$$\dot{X} = \frac{2}{3}C\dot{\varepsilon}_p - \gamma X_{\dot{p}} \tag{5}$$

$$\dot{p} = \frac{1}{h}H(f)\left\langle \frac{3}{2}\frac{(\sigma' - X') : \dot{\sigma}}{J_2(\sigma - X)} \right\rangle \tag{6}$$

$$h = C - \frac{3}{2}\gamma\frac{(\sigma' - X') : X}{J_2(\sigma - X)} + b(Q - R) \tag{7}$$

$$\dot{\varepsilon}_p = \frac{3}{2}\dot{p}\frac{\sigma' - X'}{J_2(\sigma - X)} \tag{8}$$

K, G, σ_{y}, Q, b, C, and γ are constants depending only on the used material.

H(f) is the Heaviside function: $H(f) = 0$ if $f < 0$, and $H(f) = 1$ if $f \geqslant 0$. $\langle a \rangle$ corresponds to the positive part of a.

X' and σ' are the deviators of respectively X and σ. And J_2 is the second invariant of the stress deviator.

The calculated plastic strain subtracted from the total strain in the behaviour law (2) is implemented by modifying the elastic usual behaviour law.

The Equation (3) represents the yield surface.

The Equation (4) calculates the isotropic hardening variable R.

The Equation (5) is the PDE governing the kinematic hardening tensor X.

Equations (6) and (7) describe the evolution of the accumulated plastic strain variable p.

And Equation (8) describes the evolution of the plastic strain ε_{p}.

The model parameters are identified using thin brazed sheet. The elastic parameters are identified by tensile tests. The hardening parameters are identified using a combination of nanoindentation Vickers test (across a section of the laminate) and numerical simulations with Abaqus©. Nanoindentation testing indeed yields the loading/unloading curve of the indenter corresponding to the elasto-plastic response of the material. Using a finite element simulation of the indentation test with a Chaboche model, we are able to plot the numerical loading/unloading curve that can be compared with the experimental curve. An identification procedure (BFGS algorithm) has been developed in order to find the hardening parameters that minimise the distance between the two curves. Similar procedures have been developed in published literature to link the curve parameters to the mechanical properties, see for example Dao, Chollacoop, Van Vliet, Venkatesh, and Suresh (2001).

The sum total of this procedure is that all the material parameters are identified. Figure 4 shows the two indentation curves on completion of the identification procedure.

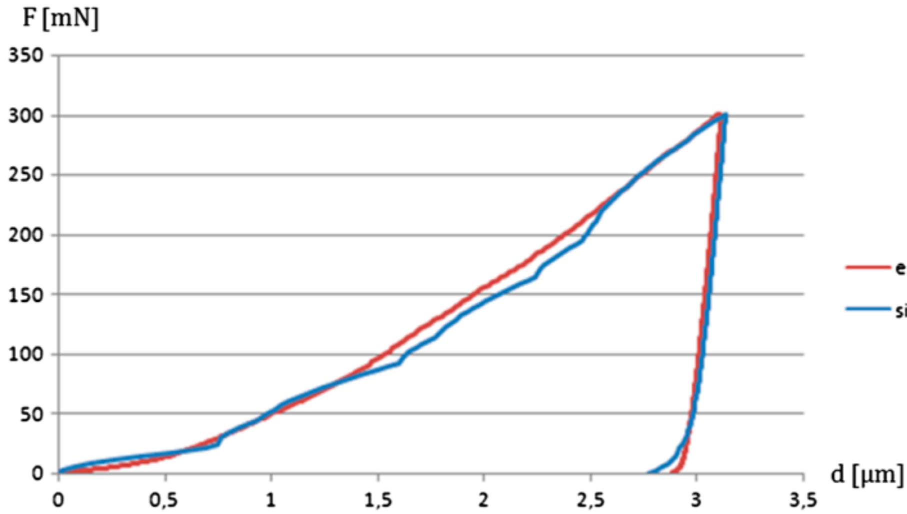

Figure 4. Experimental (blue) and numerical (red) indentation curves.

4. Mechanical cyclic response of the critical zone of the heat exchanger

Given that failure of automotive heat exchangers occurs predominantly within the inlet zone at the tube-collector junction, we decided to restrict the simulation investigation to the thermal shock response of this area.

The computational domain is illustrated in Figure 5. The thermal form of Equation (1) and the elasto-plastic model defined in Section 3 are implemented in Comsol Multiphysics© software in order to evaluate the stress/strain and plastic strain history during the thermal shock cycles.

After ten cycles of thermal shock the strain-stress cycle at the critical node stabilises and the plastic energy dissipated during a stabilised cycle can be evaluated. Figure 6 shows the evolution of the dissipated volumetric energy for three different mesh densities.

As the critical zone is located in a stress concentration zone, the evaluation of the stresses is mesh-size dependent. For this reason, we propose the use of a minimum mesh size corresponding to 1/5 of the tube thickness.

5. Lifetime prediction of the critical zone of the heat exchanger

Using an energy based lifetime criteria (Constantinescu, Charkaluk, Lederer, & Verger, 2004) identified by four-point bending tests and numerical simulation of these tests, we are able to evaluate the energy dissipated at the critical point. We have identified the criteria as presented in Equation (9).

$$W_p = \alpha (N_r)^{\beta} \tag{9}$$

W_p is the dissipated energy per cycle, N_r is the number of cycle to failure. α and β are material parameters identified using fatigue bending tests.

Figure 7 presents the steps for the identification of the fatigue criteria for the brazed aluminium composite. The fixed displacement command is similar for the experimental and simulated bending tests. From the experimental tests, we are able to count the

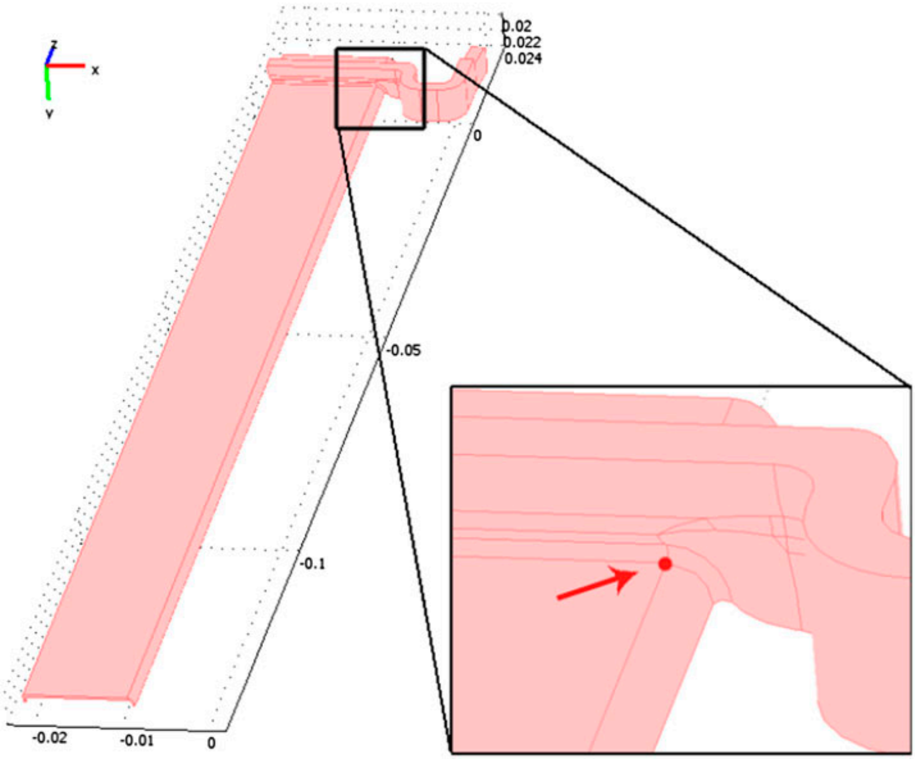

Figure 5. Tube-collector computational domain.

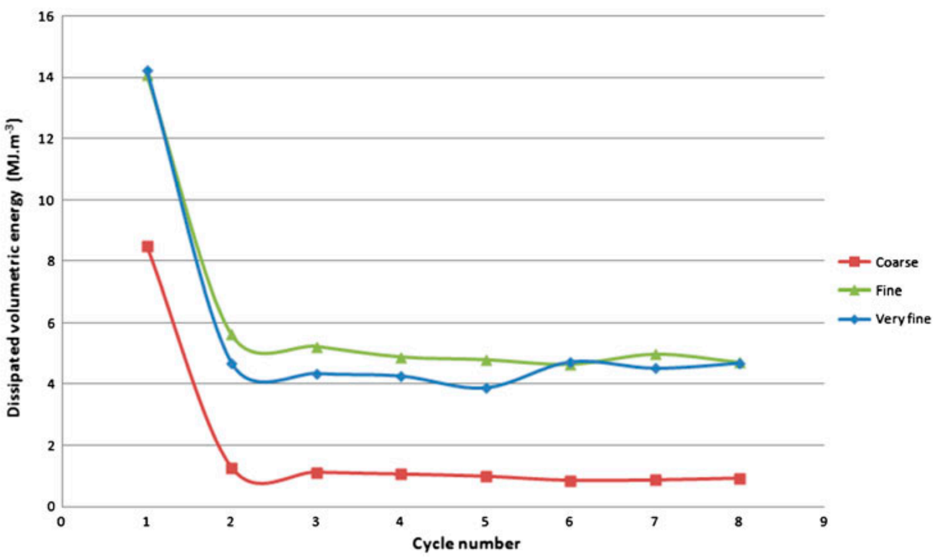

Figure 6. Evolution of the dissipated volumetric energy for three different mesh sizes.

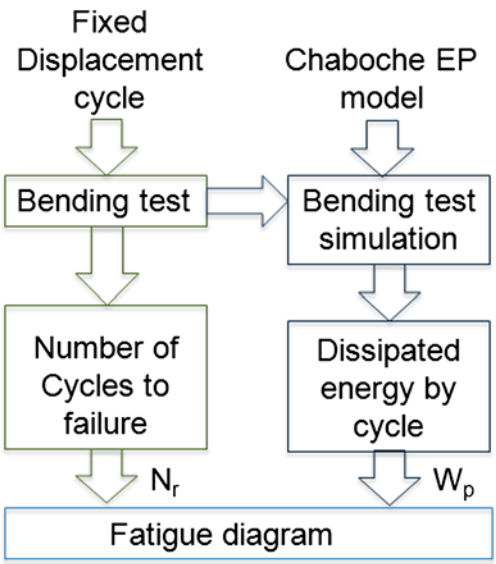

Figure 7. Identification steps of the fatigue criteria.

number of cycles to failure of the tested material, whereas from the simulations, we are able to compute the dissipated energy on the stabilised cycle. This energy depends obviously on the behaviour of the material. The elasto-plastic model defined in Section 3 was used.

The campaign of identification of the fatigue criterion of the aluminium alloys based on several displacement commands give the diagram Figure 8. Case 1 corresponds to 3916 aluminium composite with two 4045 layers as defined in the introduction. We

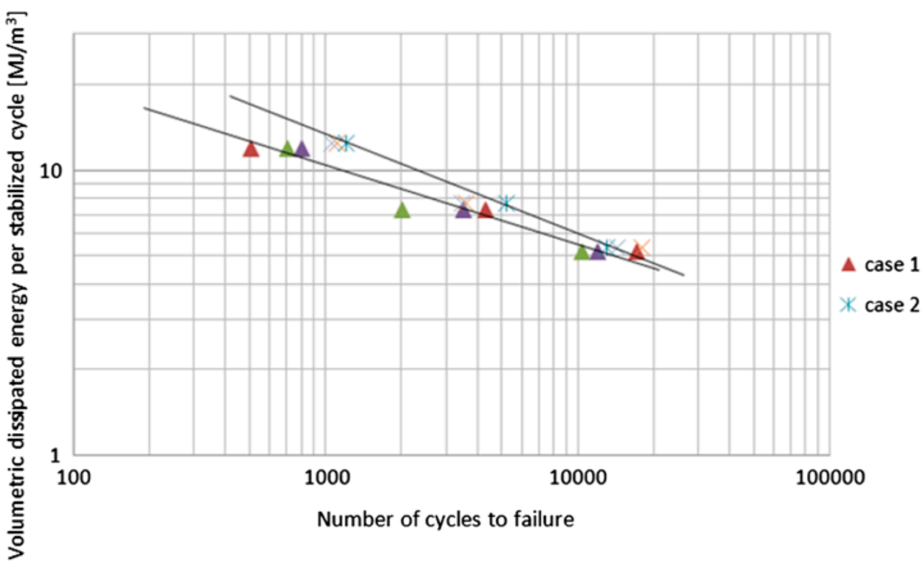

Figure 8. Identification of the fatigue criteria.

have studied the fatigue of a second brazed aluminium composite, where one of the plated layers is replaced with a 7 series aluminium alloy which has better corrosion properties. This layer is located inside the heat exchanger tubes. This new configuration is defined as case 2 in the fatigue diagram.

The simulation of a realistic geometry of the critical zone of the heat exchanger as in section 4 permits us to compute the dissipated energy on the stabilised cycle of such geometry. The lifetime estimation is then visualised on the diagram shown in Figure 8. In this study of tube-collector junction, we compute a dissipated energy of almost 5 [MJ/m^3] that gives a lifetime estimation of around 10,000 cycles. This estimation is close to the experimental observation.

6. Conclusion

We have developed a comprehensive fatigue design approach capable of estimating the lifetime of aluminium automotive heat exchangers. We have defined and identified a cyclic elasto-plastic model for the aluminium brazed laminate. Nanoindentation tests coupled with numerical simulations help us to identify the hardening parameters of the laminate. Based on infrared thermography measurements, we have proposed a form for the thermal history during the thermal shock. Combining four points bending tests and numerical simulations, we have built fatigue diagrams based on the dissipated energy during the stabilised cycle.

We have implemented the Chaboche elasto-plastic model in Comsol multiphysics© to compute the dissipated energy at the stabilised cycle at each node of the mesh. Using the identified fatigue criteria, we are then able to localise the critical zones of the heat exchanger and to estimate the lifetime.

Acknowledgement

We want to thank the French National Research Agency (ANR) for its financial contribution to this project.

References

Chaboche, J. L. (1989). Constitutive equations for cyclic plasticity and cyclic viscoplasticity. *International Journal of Plasticity, 5*, 247–302.

Constantinescu, A., Charkaluk, E., Lederer, G., & Verger, L. (2004). A computational approach to thermo-mechanical fatigue. *International Journal of Fatigue, 26*, 805–818.

Dao, M., Chollacoop, N., Van Vliet, K. J., Venkatesh, T. A., & Suresh, S. (2001). Computational modeling of the forward and reverse problems in instrumented sharp indentation. *Acta Materiala, 49*, 3899–3918.